OSCAR-based reconstruction for compressed sensing and parallel MR imaging

L. El Gueddari,[1,2] Ph. Ciuciu,[1,2,*] E. Chouzenoux[3,4], A. Vignaud[1] and J.-C. Pesquet[3,4]

[1]CEA/NeuroSpin, Univ. Paris-Saclay, Gif-sur-Yvette, France

Inria Saclay-Ile de France, Parietal, France

[3]Inria Saclay-Ile de France, Opis, Palaiseau, France

[4]CentraleSupélec, CVN, Gif-sur-Yvette, France

[*]To whom correspondence should be addressed; E-mail: philippe.ciuciu@cea.fr.

May, 14 2019

Abstract

Compressed sensing combined with parallel imaging has allowed significant reduction in MRI scan time. However, image reconstruction remains challenging and common methods rely on a coil calibration step. In this work, we focus on calibrationless reconstruction methods that promote group sparsity. The latter have allowed theoretical improvements in CS recovery guarantees. Here, we compare the performances of several regularization terms (group-LASSO, sparse group-LASSO and OSCAR) thatdefine with the data consistency term the convex but non-smooth objective function to be minimized. The same primal-dual algorithm is used to perform this minimization. Our results demonstrate that OSCAR-based reconstruction is competitive with state-of-the-art ℓ_1-ESPIRiT.

Introduction

Compressed sensing (CS) theory has made a breakthrough in Magnetic Resonance Imaging (MRI) since it has unlocked one of the major issues in MRI, namely the slow data acquisition. In the high resolution setting, CS must be combined with parallel imaging (PI) to preserve high signal-to-noise ratio, leading to harder reconstruction problems. In the existing CS-PI literature, most algorithms reconstruct a single full field-of-view MR image using a (self-) calibration step that estimates the coil sensitivity maps. In this work, we explore a new formulation based on structured group sparsity. Compared to usual mixed-norm regularization such as group-LASSO (*1*) and sparse group-LASSO (*2*), the OSCAR formulation (*3*) is implemented for the first time for CS-PI image reconstruction. On prospective non-Cartesian CS-PI 7T data, we show that our approach reaches similar image quality to ℓ_1-ESPIRIT

Theory

General problem statement. Let N, L and M being respectively the image resolution, the number of channels and the number of k-space measurement. We denote $\boldsymbol{y} = [\boldsymbol{y}_1, \ldots, \boldsymbol{y}_L] \in \mathbb{C}^{M\times L}$ the acquired NMR signal and $\underline{\boldsymbol{x}} = [\boldsymbol{x}_1, \ldots, \boldsymbol{x}_L] \in \mathbb{C}^{N\times L}$ be the reconstructed MR images. The image reconstruction problem reads as follows:

$$\widehat{\underline{\boldsymbol{x}}} = \underset{\underline{\boldsymbol{x}}\in\mathbb{C}^{N\times L}}{\arg\min}\Big\{\frac{1}{2}\sum_{\ell=1}^{L}\sigma_\ell^{-2}\|f_\Omega(\boldsymbol{x}_\ell) - \boldsymbol{y}_\ell\|_2^2 + g(\boldsymbol{T}\underline{\boldsymbol{x}})\Big\}, \quad (1)$$

where f_Ω is the forward under-sampling Fourier operator. $\boldsymbol{T} \in \mathbb{C}^{N_\Psi\times N}$ is a linear operator related to a multiscale decomposition $\Psi \in \mathbb{C}^{N_\Psi}$ and g is the joint sparsity promoting term.

Group LASSO.

We define $\underline{\boldsymbol{z}} = [\boldsymbol{z}_1, \ldots, \boldsymbol{z}_L] \in \mathbb{C}^{N_\Psi\times L}$, with $\boldsymbol{z}_\ell \in \mathbb{C}^{N_\Psi}$ the wavelet coefficients composed of S sub-bands having P_s coefficients each. For $\underline{\boldsymbol{z}} \in \mathbb{C}^{N_\Psi\times L}$, the group-LASSO regularization is given by:

$$g_{\mathrm{GL}}(\underline{\boldsymbol{z}}) = \|\underline{\boldsymbol{z}}\|_{1,2} = \sum_{s=1}^{S}\left(\lambda\gamma^{s_c}\sum_{p=1}^{P_s}\sqrt{\sum_{\ell=1}^{L}|z_{sp\ell}|^2}\right) \quad (2)$$

where $z_{sp\ell}$ is the p^{th} wavelet coefficient of the s^{th} sub-band (in the s_c-scale) for the ℓ^{th} coil. For a given s and p, the proximity operator reads:

$$\left(\mathrm{prox}_{\lambda\gamma^{s_c}\|\cdot\|_{1,2}}(\underline{\boldsymbol{z}})\right)_{sp\ell} = \begin{cases} z_{sp\ell}\left(1 - \frac{\lambda\gamma^{s_c}}{\alpha_{sp}}\right) & \text{, if } \alpha_{sp} \geq \lambda\gamma^{s_c} \\ 0 & \text{, otherwise} \end{cases} \quad (3)$$

with $\alpha_{sp} = \sqrt{\sum_{\ell=1}^{L} |z_{sp\ell}|^2}$. The hyper-parameters $\lambda > 0$ and $\gamma > 0$ enables a s_c-scale dependent regularization according to a power-law behavior (*4*).

Sparse group-LASSO. On top of inter-group sparsity, the sparse group-LASSO imposes intra-group sparsity too:

$$\forall \underline{\boldsymbol{z}} \in \mathbb{C}^{N_\Psi \times L}, g_{\mathrm{sGL}}(\underline{\boldsymbol{z}}) = g_{\mathrm{GL}}(\underline{\boldsymbol{z}}) + \mu \left\|\underline{\boldsymbol{z}}\right\|_1 \tag{4}$$

The proximity operator of g_{sGL} corresponds to the composition of the proximity operator of the group-LASSO Eq. (3) and the soft-thresholding as established in (*2*).

Octogonal Shrinkage and Clustering Algorithm for Regression. Instead of using the ℓ_2 norm to define the groups, one can infer a group structure using a pairwise ℓ_∞ norm while imposing the ℓ_1 norm as a sparsity constraint. This leads to the OSCAR regularization that reads as follows:

$$\begin{aligned} g_{\mathrm{OSCAR}}(\boldsymbol{z}) &= \sum_{s=1}^{S} \lambda \left[\sum_{j=1}^{P_s L} |z_{sj}| + \gamma \sum_{j<k} \max\{|z_{sj}|, |z_{sk}|\} \right] \\ &= \sum_{s=1}^{S} \lambda \left[\sum_{j=1}^{P_s L} \left(\gamma(j-1)+1\right) |z_{sj}|_\downarrow \right] \end{aligned} \tag{5}$$

where $\underline{\boldsymbol{z}}_\downarrow \in \mathbb{C}^{N_\Psi \times L}$ is the inter sub-band and channels wavelet coefficients sorted in decreasing order , i.e.: $\forall s \in \mathbb{N}, |z_{s1}| \leq \cdots \leq |z_{sP_sL}|$. The proximity operator is also explicit (*5, Eq. (24)*).

Primal-dual optimization algorithm. To solve the image reconstruction problem, we implemented the primal-dual optimization method proposed by Condat-Vú (*6, 7*) and summarized Fig. 1. As all these penalty terms are prox-friendly, one can also use any proximal splitting algorithm.

Experiments & Results

Acquisition parameters. A modified 2D T2*-weighted GRE sequence (*8*) composed of 34 spokes (acceleration factor of 15 in time) and 3072 samples each (under-sampling factor of 2.5).

The acquisition parameter were set as follows: FOV= 200×200mm^2, slice thickenss of 3mm, TR = 550ms (for 11 slices), TE= 30ms, BW=100kHz and FA= $25°$.

Reconstruction parameters. All the hyper-parameters were set using a grid search procedure and the undecimated bi-Orthogonal wavelet transform with 4 scale of decomposition was used as sparsifying transform. We compared the Sum-Of-Squares for the gLASSO, sgLASSO and OSCAR regularizations.

Results & Discussion.

Fig. 2 compares the results of the SOS for the different penalizations, in terms of SSIM and image quality. It suggests that the group structure is more important than the intra group sparsity since OSCAR performs better.

Fig. 4 shows the coil-by-coil images, the structure is better preserved by the OSCAR regularization at the expense of low SNR valuue as seen on Fig. 3 (first row)

Conclusion

Since the results are equivalent for OSCAR and the ℓ_1-ESPIRiT solution this tends to prove that the information of sensitivity is inferred via a well-suited group structure. Moreover reconstruction based on group-sparsity promotion achieve tighter recovery guarantee (*9*). OSCAR regularization tends to spread the SSIM scores of coil specific MR images whereas the group-LASSO and its sparse variation are more concentrated.

Figures

Algorithm 1: Condat-Vú algorithm

initialize $k = 0, \tau > 0, \kappa > 0, \underline{\boldsymbol{x}}_0, \underline{\boldsymbol{z}}_0$;
while $k \leq K$ **do**
  $\underline{\boldsymbol{x}}_{k+1} := \underline{\boldsymbol{x}}_k - \tau \left(\nabla f(\underline{\boldsymbol{x}}_k) + \boldsymbol{T}^* \underline{\boldsymbol{z}}_k\right)$;
  $\underline{\boldsymbol{w}}_{k+1} := \underline{\boldsymbol{z}}_k + \kappa \boldsymbol{T} \left(2\underline{\boldsymbol{x}}_{k+1} - \underline{\boldsymbol{x}}_k\right)$;
  $\underline{\boldsymbol{z}}_{k+1} := \underline{\boldsymbol{w}}_{k+1} - \kappa \operatorname{prox}_{g/\kappa} \left(\frac{\underline{\boldsymbol{w}}_{k+1}}{\kappa}\right)$;
end

Figure 1: Condat-Vù algorithm. The hyper-parameter were set as follow, $\tau := \frac{1}{\beta}$, $\kappa := \frac{\beta}{2\|\boldsymbol{T}\|^2}$ with β the Lipschitz constant of the norm of f_Ω.

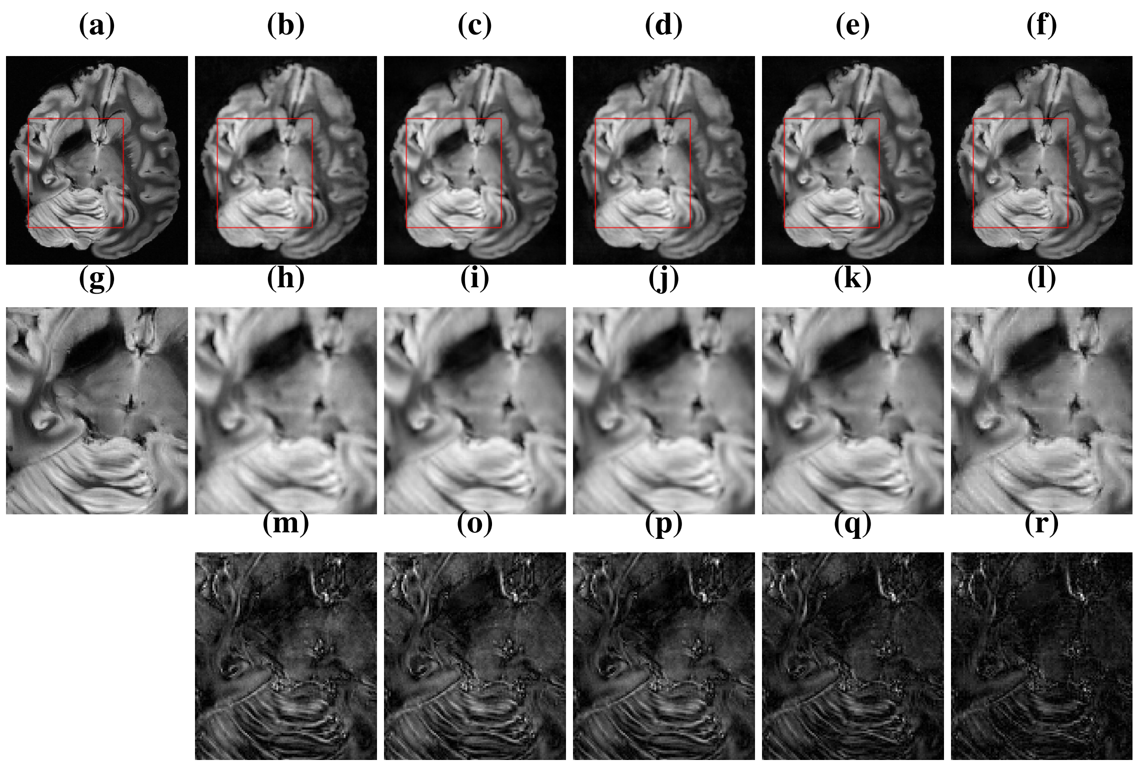

Figure 2: **(a)** Cartesian reference. **(b)** Reconstruction with no regularization term (SSIM $= 0.847$, pSNR $= 26.50$). **(c)** Reconstruction based on the group-LASSO penalty (SSIM $= 0.864$, pSNR $= 26.92$). **(d)** Reconstruction based on the sparse group-LASSO penalty (SSIM $= 0.851$, pSNR $= 26.77$). **(e)** Reconstruction based on OSCAR penalty (SSIM $= 0.875$, pSNR $= 30.49$) **(f)** reconstruction based on ℓ_1-ESPIRiT (SSIM $= 0.874$, pSNR $= 28.32$). **(g)-(l)** Respective zooms in the red square, **(m)-(r)** zoom of the difference between the Cartesian referance and the reconstructed image.

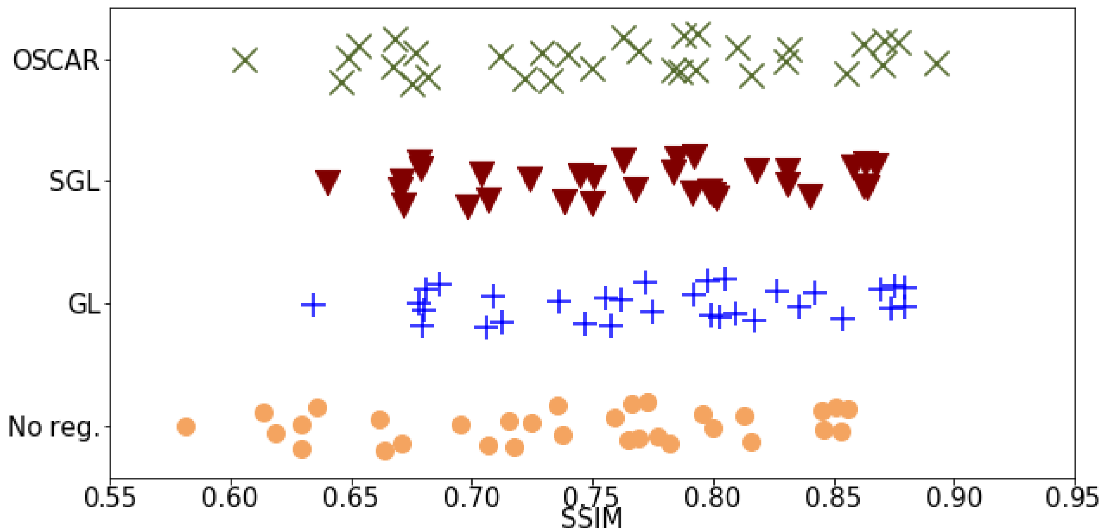

Figure 3: Assessment of the SSIM score per channel.

References and Notes

1. A. Majumdar and R. Ward, "Calibration-less multi-coil MR image reconstruction," *Magnetic Resonance in Medicine*, vol. 30, no. 7, pp. 1032–1045, 2012.

2. J. Friedman, T. Hastie, and R. Tibshirani, "A note on the group lasso and a sparse group lasso," *arXiv preprint arXiv:1001.0736*, 2010.

3. H. Bondell and B. Reich, "Simultaneous regression shrinkage, variable selection, and supervised clustering of predictors with OSCAR," *Biometrics*, vol. 64, no. 1, pp. 115–123, 2008.

4. N. Pustelnik, A. Benazza-Benhayia, Y. Zheng, and J.-C. Pesquet, *Wavelet-Based Image Deconvolution and Reconstruction*, pp. 1–34, American Cancer Society, 2016.

5. Z. X. and M. Figueiredo, "The ordered weighted l1 norm: Atomic formulation, projections, and algorithms," *arXiv preprint arXiv:1409.4271*, 2014.

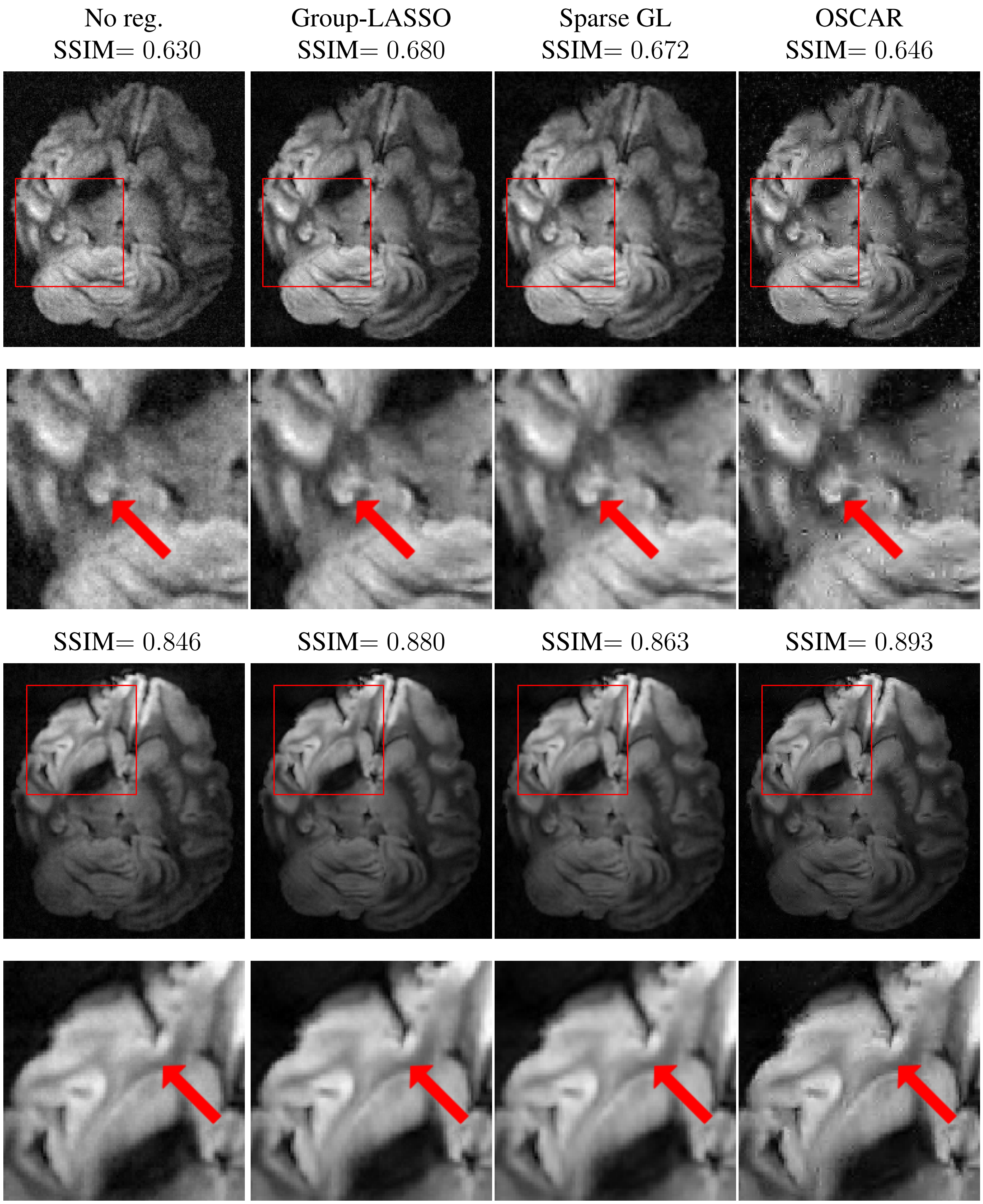

Figure 4: From left to right, no penalization, group-LASSO solution, sparse group-LASSO and OSCAR solutions for two different channels (each row represent a different channel), the first row is a low SNR.

6. L. Condat, "A primal–dual splitting method for convex optimization involving lipschitzian, proximable and linear composite terms," *Journal of Optimization Theory and Applications*, vol. 158, no. 2, pp. 460–479, Aug 2013.

7. B. Vũ, "A splitting algorithm for dual monotone inclusions involving cocoercive operators," *Advances in Computational Mathematics*, vol. 38, no. 3, pp. 667–681, Apr 2013.

8. C. Lazarus, P. Weiss, N. Chauffert, F. Mauconduit, L. El Gueddari, C. Destrieux, I. Zemmoura, A. Vignaud, and P. Ciuciu, "Variable-density k-space filling curves for accelerated Magnetic Resonance Imaging," 2018.

9. I. Chun, B. Adcock, and T. Talavage, "Efficient compressed sensing SENSE pMRI reconstruction with joint sparsity promotion," *IEEE transactions on Medical Imaging*, vol. 35, no. 1, pp. 354–368, 2016.